ADAPTABLE AND REUSABLE DOUBLE-SIDED BEAM-TO-BEAM STEEL JOINT

Neda Janković[a], Filip Ljubinković[a], Jorge Conde[b] and Luís Simões da Silva[a]

[a] *Universidade de Coimbra, ISISE, ARISE, Departamento de Engenharia Civil, Portugal.*
[b] *Universidad Politécnica de Madrid, Departamento de Física y Estructuras de Edificación, Spain.*

Abstract: With growing demands for sustainability and circularity in the construction sector, enhancing the reusability of steel components has become a key priority. The European CONNECT4C project addresses this challenge by developing innovative, adaptable steel components that enable flexible and reusable structural systems. This paper investigates newly developed moment-resisting double-sided beam-to-beam steel joints, focusing on the preparation of the experimental campaign and a preliminary numerical study. The aim is to assess the joint's moment resistance, rotational stiffness, ductility, deformation capacity, and failure mechanisms.

1. Introduction

One of the most pressing global challenges is the reduction of CO_2 emissions, with the construction sector alone responsible for approximately 39% of global emissions [1]. To address this, the transition toward a circular economy has become a central strategy, emphasising the need for demountable and reusable construction solutions. Steel, as a highly durable and recyclable material, has strong potential to contribute to this transition. However, despite these advantages, the direct reuse of steel remains limited [2]. Within this context, structural connections play a decisive role. Not only do they account for nearly half of the total construction costs, but they also determine the practicality of disassembly and reassembly processes [3]. The CONNECT4C project [4] builds on previous research projects [5,6] by advancing the development of innovative, adaptable, and demountable connections that extend the scope of reuse in steel structures. Fig. 1 illustrates the project's conceptual framework: bolted connections are designed to enable straightforward disassembly, while additional components are integrated to allow for future adaptation and extended service life.

The present study forms part of the CONNECT4C project and focuses on the development of adaptable, reusable beam-to-beam moment-resisting joints capable of accommodating large tolerances. Such joints are designed for use in various building configurations, thereby extending reuse opportunities and contributing to the realisation of circular construction practices.

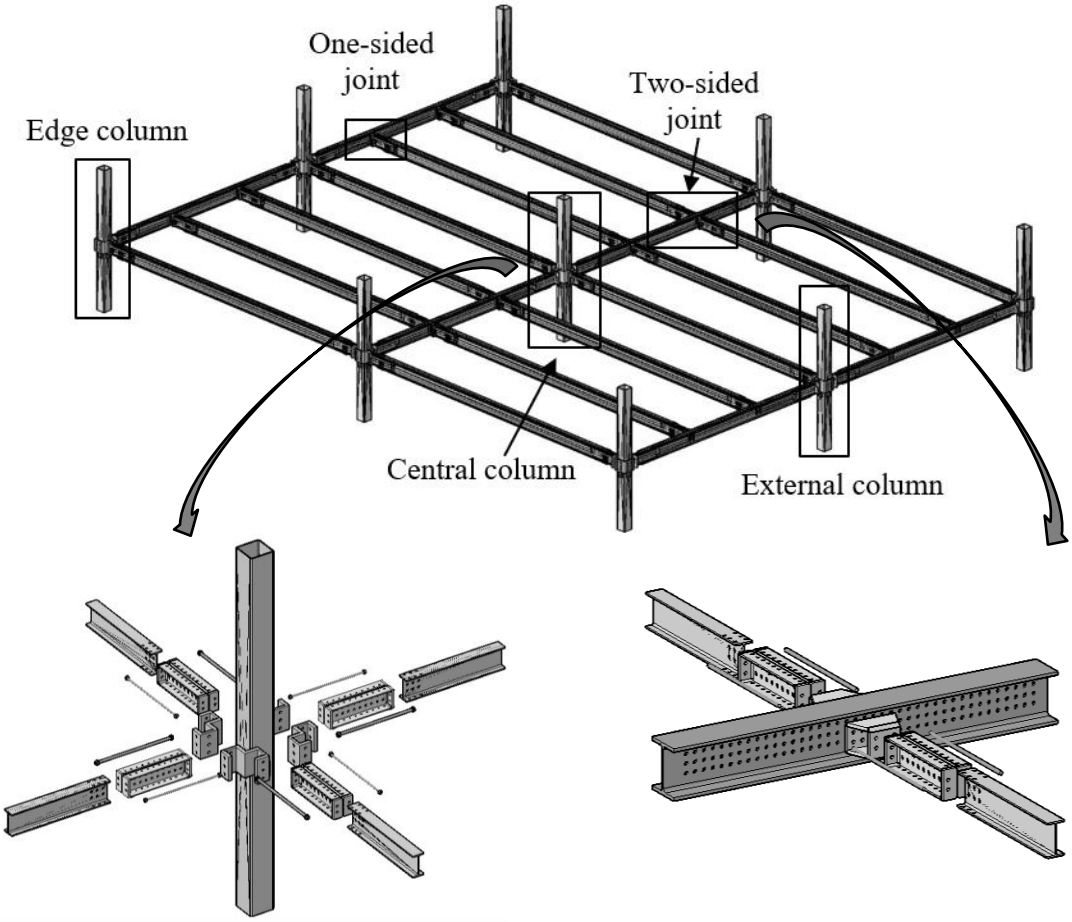

Fig. 1: Conceptual sketch of C4C structural system [4].

2. Adaptable joint

The adaptable two-sided joint investigated in this study consists of two secondary beams (joists) connected to a main beam. To achieve demountability and reuse, only the mechanical fasteners are used, with no welding. To enable full adaptability, a modular perforation grid of 75 mm is adopted across all components, allowing the joint to accommodate varying beam lengths and positions with incremental adjustments. The overall concept of the connection is illustrated in Fig. 2.

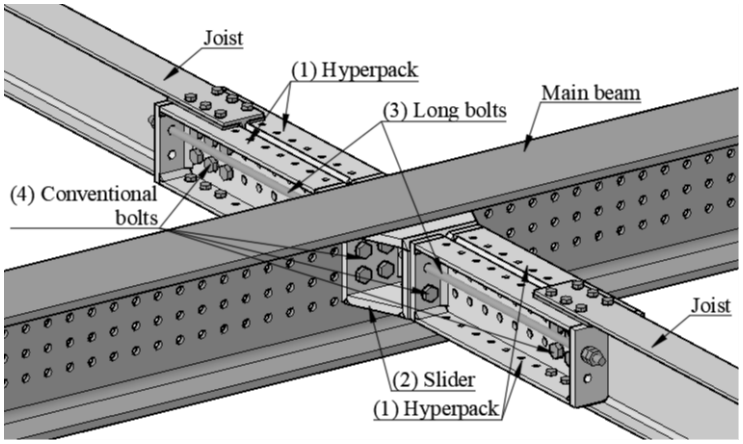

Fig. 2: Adaptable beam-to-beam joint.

The connection between a single joist and the main beam is achieved by several carefully designed pieces: (1) two hyperpacks, (2) one slider, (3) two long bolts, and (4) three groups of conventional bolts, connecting the hyperpacks and the joist, the hyperpack and the slider, as well as the slider and the main beam. The hyperpack is a prismatic element composed of five plates welded together, as shown in Fig. 3. It is perforated along its length with a discrete 75 mm hole grid, which enables joist-to-hyperpack connections at virtually any location, providing large horizontal adaptability for the joists. Consequently, different joist lengths can be used to span the same distance between the two main beams. This drastically reduces the stocking needs for reclaimed elements, allowing for approximately 1 m tolerance in profile length requirement. To address assembly challenges from the joist's radius, packing plates are employed to ensure proper fit (see Fig. 3(c)).

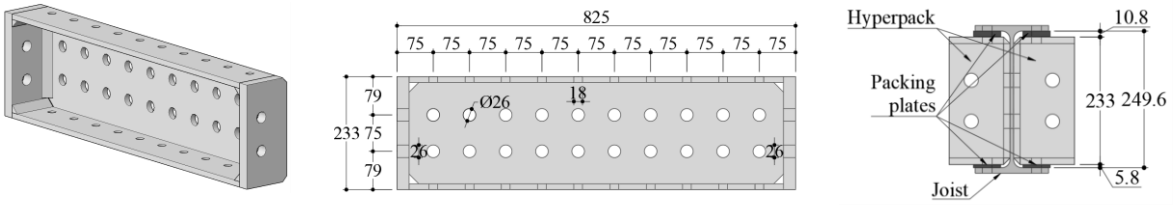

(a) Isometric view (b) Dimensions (c) Packing plates

Fig. 3: Hyperpack.

The slider is a piece that links the hyperpack to the main beam. Two distinct configurations are studied hereafter: the small and the big sliders. The small slider aligns with the joist and hyperpack height, utilising a configuration of long bolts for moment transfer. The long bolts are designed to carry tensile forces, while compressive forces are transmitted directly through bearing contact at the opposite end of the slider-hyperpack interface. This arrangement creates a force couple, with the distance between the tension zone (bolts) and the compression zone (contact surface) acting as a lever arm, thereby allowing the joint to resist and transfer bending moments effectively. Additionally, standard bolts are used for shear transfer (see Fig. 4(a), (c)). The height of the big slider matches the main beam depth and incorporates a welded shear key beneath the joist to assume the primary role in shear transfer (see Fig. 4(b), (d)).

However, two alternative bolt configurations are investigated for both sliders: (i) the first, original, configuration consists of one row of long bolts combined with one row of conventional bolts (referred to as 'T1a' and 'T2a' in the results section), and (ii) the second replaces the conventional bolts with an additional row of long bolts (referred to as 'T1b' and 'T2b'). The introduction of an additional long bolt row is intended to enhance the moment resistance of the connection. These alternatives have been numerically assessed, and the findings are reported later in this paper.

Both slider configurations are designed with bolt holes following the 75 mm grid (see Fig. 4 (e), (f)), ensuring compatibility with the overall system and allowing assembly at any position within the main beam's web. To ensure that stress ranges remain within the elastic domain, and hence enable their reusability, both the hyperpack and the slider are made in high-strength steel S690.

All connections within the joint are bolted, combining standard preloaded bolts in accordance with EN 14399 [7] with long bolts. As highlighted in [8], achieving shank fracture of the long bolts, rather than thread stripping, provides a more ductile and thus desirable failure mode. To preclude thread stripping, the use of double HV nuts during assembly is recommended. The beam-slider connection is solved with conventional preloaded bolts, with four bolts per row to ensure friction-resistance at the ultimate limit state, thus avoiding bearing damage in the main beam. This is also the case in the joist-hyperpack connection.

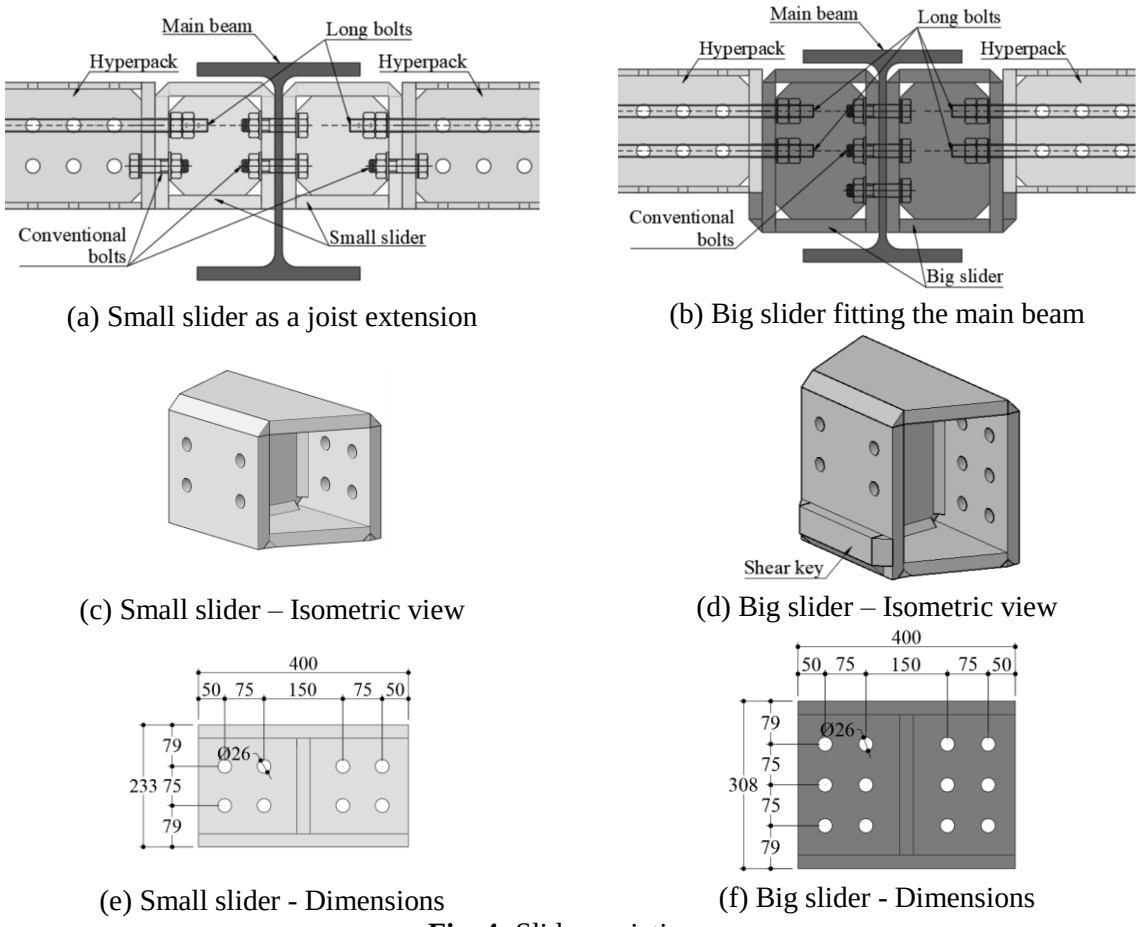

(a) Small slider as a joist extension

(b) Big slider fitting the main beam

(c) Small slider – Isometric view

(d) Big slider – Isometric view

(e) Small slider - Dimensions

(f) Big slider - Dimensions

Fig. 4: Slider variations.

3. Experimental campaign preparation

3.1 Test objective

Given the complexity of the proposed joint, comprising three distinct connections: (i) between the joist and the hyperpack, (ii) between the hyperpack and the slider, and (iii) between the slider and the main beam, it is essential to clearly define the objectives of the experimental tests. The primary aim of the two tests described herein is to investigate and verify the performance of the second connection, namely, the interface between the hyperpack and the slider, while checking the integrity of the third one. To isolate this connection, only a short segment of the joist is included in the test setup. This approach allows for focused observation of the bending moment and shear force transfer capacity across the hyperpack-slider interface. Four experimental tests are planned: two employing the small slider (T1a - including one long bolt and one conventional bolt row, and T1b including two long bolt rows) and the other two employing the big slider (T2a - including one long bolt and one conventional bolt row, and T2b including two long bolt rows).

3.2 Testing layout

The experimental setup is illustrated in Fig. 5. The main beam (203) is centrally positioned within the reaction frame (101). A 3 MN hydraulic jack, mounted on the reaction frame (101),

applies a vertical load directly onto the main beam (203). This represents a simplified inversion of the actual loading scenario where, in reality, the load would be applied to the joists (204) rather than the main beam. In this experimental setup, the system is effectively turned upside-down to facilitate load application and measurements. The guiding system (110) ensures that the beam can move downward in a controlled, linear fashion during loading.

On both sides of the beam, the joists (204) are supported using pinned supports (106, 107). These supports restrict vertical displacements while permitting rotation around axes perpendicular to the beam. The slotted pin, equipped with integrated hinges, is designed to theoretically prevent out-of-plane displacements.

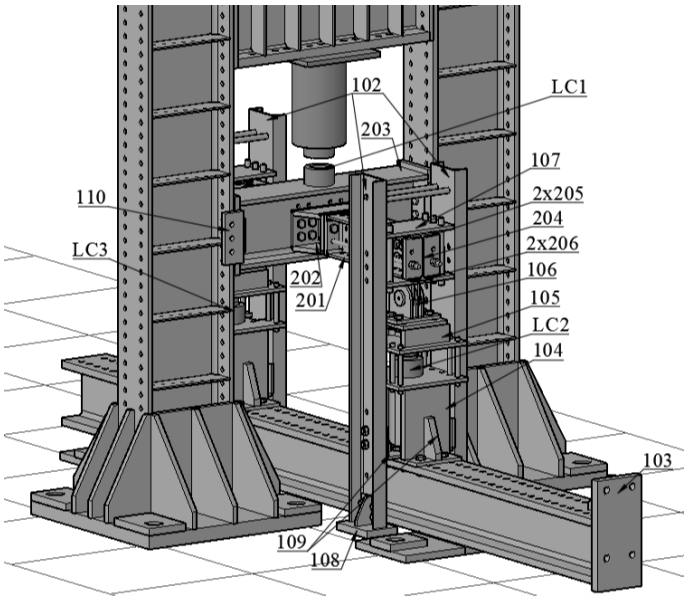

Fig. 5: Experimental layout of the two-sided test.

For additional control and safety, lateral restraints (102) are incorporated to eliminate any potential out-of-plane movements. These restraints are connected via two rods at their top ends to maintain a fixed spacing, ensuring system stability. Importantly, the restraints are fixed to the structure only below the load cells (LC2 and LC3) which are assembled between their supporting parts (104 and 105). This layout is designed to ensure precise load application and accurate measurement, while minimising unwanted effects and uncontrolled degrees of freedom. Another load cell (LC1) is positioned on the main beam (203), directly below the hydraulic jack, to capture the direct force applied.

4. Numerical modelling

4.1 Overview

According to the planning outlined in the previous chapter, four physical tests are scheduled for the two-sided beam-to-beam joint, with the variables being the geometry of the slider and bolt configuration. To support and replicate these experiments, preliminary Abaqus finite element models have been developed. In total, four numerical models were developed to examine these variations (see Fig. 6), and their details are summarised in Table 1.

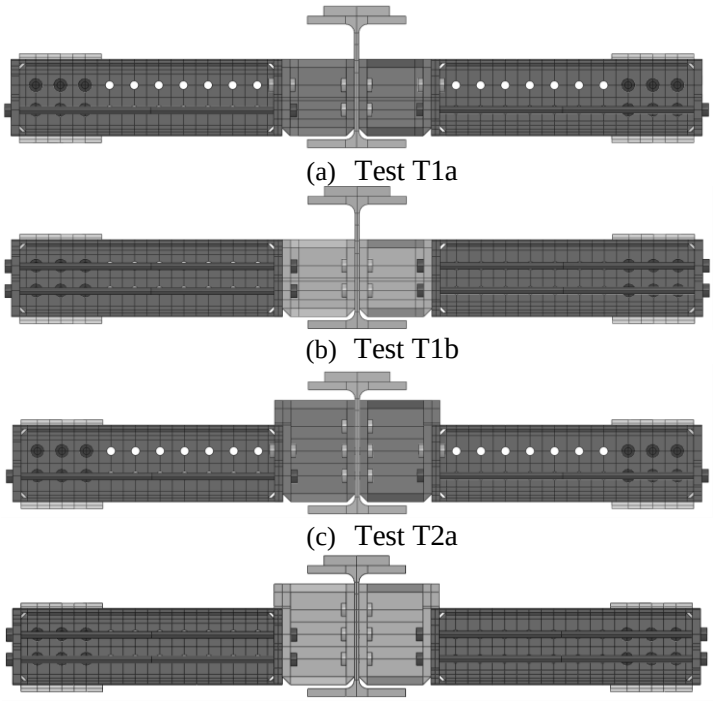

(a) Test T1a

(b) Test T1b

(c) Test T2a

(d) Test T2b

Fig. 6: Studied numerical models.

Table 1: Summary of the studied models.

Test	Slider type	Long bolt rows	Conventional bolt rows	Figure
T1a	Small	1	1	Fig. 6(a)
T1b	Small	2	0	Fig. 6(b)
T2a	Big	1	1	Fig. 6(c)
T2b	Big	2	0	Fig. 6(d)

4.2 Modelling details

As shown in Fig. 6, the test setup features the beam-to-beam joint in an inverted position compared to its actual orientation in service. This inversion is intentional and was adopted to facilitate testing, allowing the load to be applied directly onto the main beam, while the joists are provided with pinned supports. This configuration enables simplified and more precise control of the applied load during the experiment.

The Abaqus models have been developed to accurately reflect this test setup. In the simulations, the load is applied as a concentrated force at the load application plate. The joists are modelled with pinned supports, and lateral movement of the main beam is fully restrained, replicating the boundary conditions of the experimental setup (see Fig. 7).

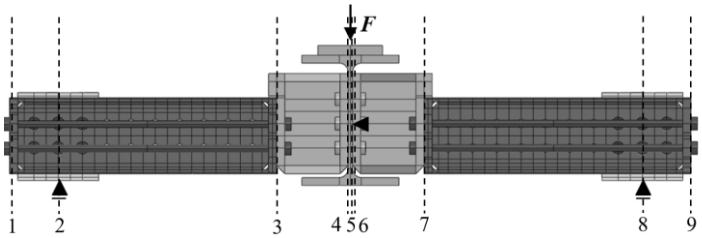

Fig. 7: Load application, boundary conditions and defined planes for bending moments diagram.

All bolts employed in the joint are M24 and are represented in the numerical models using a simplified geometry. The bolt threads are omitted, and the tensile stress area is adopted for the cross-sectional representation, consistent with common practice in numerical simulations of bolted joints. To account for preloading conditions, bolts located within the splice and those connecting the slider to the main beam are assumed to be fully preloaded, in accordance with the provisions of EN 1993-1-8 [9] ($F_{p,C}$ = 247.1 kN). Conversely, both the long bolts and the conventional bolts, connecting the hyperpack to the slider, are modelled as non-preloaded, thereby reflecting the actual boundary conditions anticipated during the experimental campaign. The friction coefficient assumed in the model is 0.35.

The structural members and connection components are assigned material properties consistent with the physical system. The main beam and joists are modelled in steel grade S355, while the hyperpacks use high-strength steel grade S690, and all bolts are grade 10.9. A quadlinear stress-strain law is adopted to capture elastic, plastic, and strain-hardening behaviour. For S355 steel, 10% overstrength is considered, whereas the S690 model is calibrated against coupon tests. This ensures that the simulations accurately reflect the mechanical response of the high-strength steel and enhance its reliability. The bolts are modelled with a bilinear constitutive law, calibrated against experimental data from a previous campaign on long bolts [8].

An overview of the material properties adopted for the numerical models is reported in Table 2.

Table 2: Steel properties.

Property	Label	Unit	Steel		
			S355	S690	10.9
Yielding strength	f_y	MPa	390.5	773.4	1101.0
Ultimate strength	f_u	MPa	539.0	822.6	1177.9

4.3 Preliminary results

The results are systematically presented for all four test configurations and include the following key output categories:

1. Load-displacement (F-u) curves: representing the relationship between the applied load on the main beam and the corresponding vertical displacements of the main beam, provide insight into the global stiffness and deformation behaviour of the system.
2. Bending moment diagram (M): along the joist direction, showing the distribution on both sides of the central main beam at the final loading increment.
3. Bolt force-displacement (F_{bolt}-u) curves: evaluation of bolt performance in the slider-hyperpack interface.
4. Moment-rotation (M-$\Delta\varphi$) curves: determination of whether the components of the joint behave as rigid bodies or instead exhibit significant deformability, while also providing insight into the relative openings between them.
5. Plasticity distribution: assessment of the potential plastic strain in joint parts.

4.3.1 Load-displacement curves

The load-displacement (F-u) curves for all four numerical models are presented in Fig. 8(a). Increasing the size of the slider, from small to big, leads to a significant improvement the initial stiffness. Interestingly, F-u curve of the test T2b, which features the big slider combined with two rows of long bolts, corresponds very well with the test T1a (small slider with the original bolt configuration). However, it demonstrates slightly greater ductility in the later stages of the

response, indicating an enhanced ability to sustain deformation without a significant loss in load-carrying capacity.

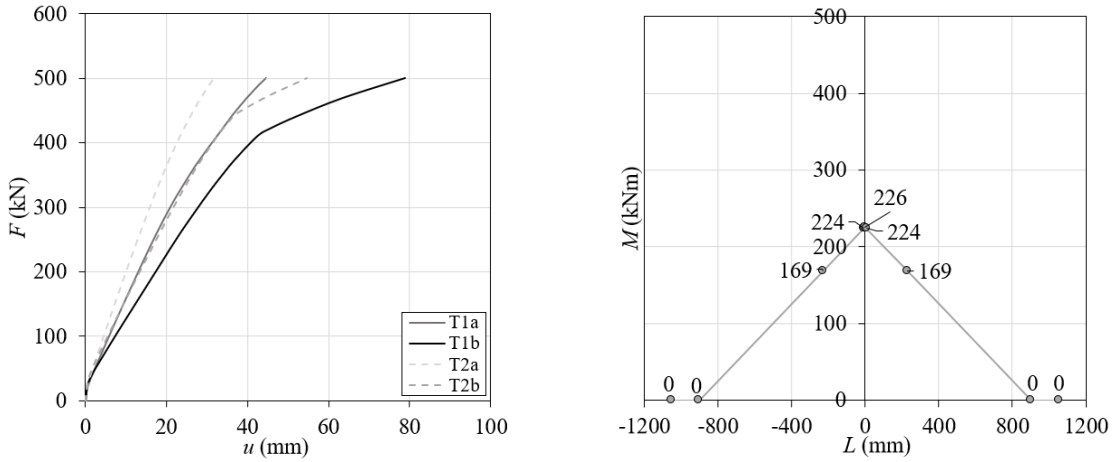

(a) *F*-*u* curves (b) *M* diagram

Fig. 8: Results - Part 1.

4.3.2 Bending moment diagram

Fig. 8(b) presents the bending moment (*M*) distribution at the final analysis increment, corresponding to an applied load of 500 kN. Each marker denotes the moment in a specific plane, as defined in Fig. 7, with the maximum moment transferred to the main beam reaching 226 kNm, across all tests.

4.3.3 Bolt force-displacement

Fig. 9(a) presents the bolt force-displacement (F_{bolt}-u) curves, showing the evolution of tensile forces in individual bolts with increasing applied load, depending on the vertical displacement of the main beam. Solid lines represent the mandatory long bolts (LB / LB1) present in all models, short-dashed lines correspond to conventional bolts (CB) beneath the LB row, and long-dashed lines indicate the second LB row included tests T1b and T2b (LB2). Two reference lines are provided: the nominal tensile resistance of M24 bolts per EN 1993-1-8 [10] ($F_{t,Rd}$ = 254 kN) and the mean experimental tensile resistance of the M24 10.9 long bolts ($F_{t,real}$) from the prior C4C testing [9]. While long bolts are mainly in tension, shear effects reduce their effective resistance compared to the theoretical tensile capacity.

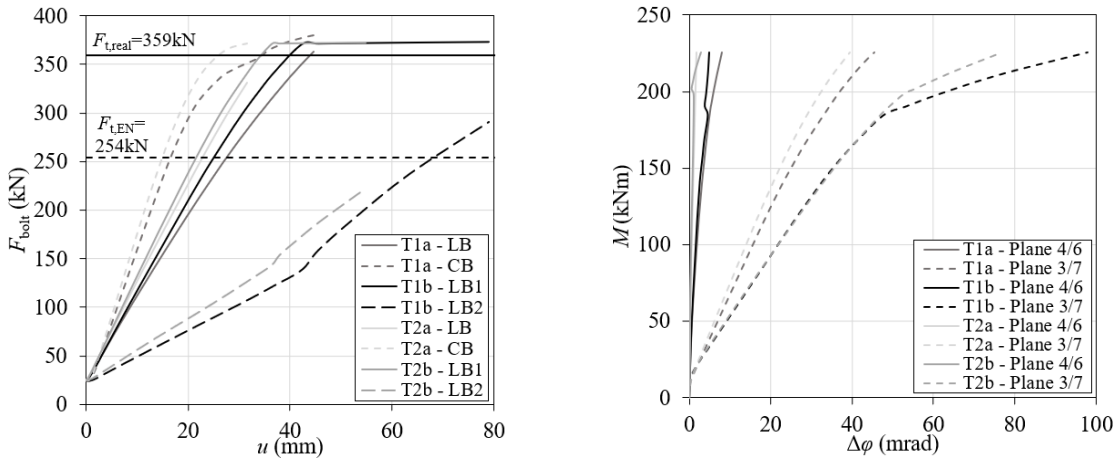

(a) F_{bolt}-u curves (b) M-$\Delta\varphi$ curves

Fig. 9: Results - Part 2.

Test comparisons highlight distinct behaviours:

- Tests T1a and T2a: Tensile forces develop simultaneously in both LBs and CBs, with the CBs carrying higher tensile forces at the same load level.
- Tests T2a and T2b: The second row of long bolts (LB2) becomes engaged as the first row approaches its capacity, thereby enhancing ductility and reducing the risk of brittle failure.

4.3.4 Moment-rotation curves

Fig. 9(b) shows the relationship between relative rotation and the bending moment in the main beam, evaluated in two planes: (i) Plane 4 (= Plane 6), representing the rotation between the web of the main beam and the slider, and (ii) Plane 3 (= Plane 7), representing the relative rotation at the slider-hyperpack interface. The results reveal a pronounced difference in rotation at the slider-hyperpack interface, indicating the presence of an opening between these components. In contrast, only minor rotations are observed in Planes 4 and 6. Overall, the results indicate that the connected elements largely behave as rigid bodies.

4.3.5 Plasticity distribution

To enable reusability of these joints, it is essential to verify that no significant damage develops in the main components. For this reason, the hyperpack and slider are fabricated from high-strength steel to ensure durability and minimise the risk of permanent deformation. Fig. 10 illustrates the plastic strain distribution in both components for test T1a. Plastic strains of approximately 1% are observed only in the compression zone between the hyperpack and slider, and only at the final stage of the analysis, after bolt failure has already occurred. This limited and localised strain suggests that both components remain largely undamaged, supporting the initial assumption of their reuse.

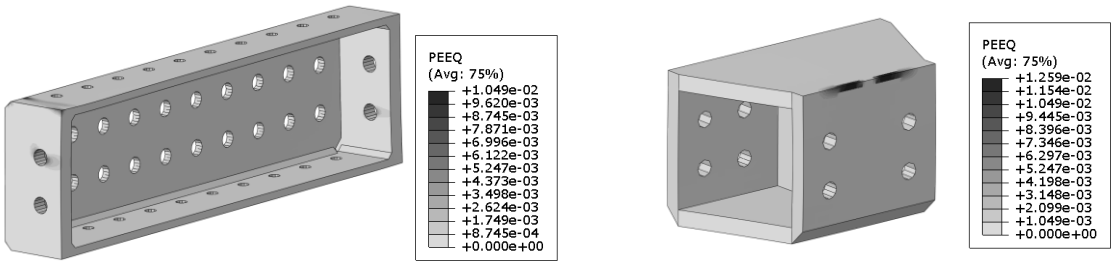

(a) Hyperpack (b) Slider

Fig. 10: Plastic strain in test T1a.

5. Summary and Conclusions

This study presented the preliminary investigation of innovative adaptable two-sided beam-to-beam moment-resisting joint, forming the basis for upcoming experimental testing. Given the complexity of the proposed connection, particular attention is given to the interaction between the newly introduced components, the slider and the hyperpack, assembled with both, long and conventional bolts.

Four physical tests will be carried out: two with a small slider and two with a big slider, and with two bolt configurations: (i) LB and CB rows and (ii) two LB rows. Numerical models are made in Abaqus to verify future experimental tests. The analyses highlighted the bolts as the most critical elements, consistently reaching their tensile resistance under the applied loads. This confirms that bolt failure is expected to occur first during testing, in line with the test's objective of assessing the capacity and performance of long bolts as the primary load-bearing components. Furthermore, all joint components behave as rigid elements, while the hyperpack

exhibited the highest degree of rotation. As the hyperpack and slider remain largely within the elastic deformation range, their reuse appears feasible, though this will be validated through the upcoming experimental testing.

Acknowledgments

This work was partly financed by:
• The European Commission's Research Fund for Coal and Steel through the research project CONNECT4C (High-strength steel connections for circular construction), ref. no. 101112300, is highly acknowledged. Disclaimer: "Work is funded by European Union. Views and opinions expressed are however, those of the author(s) only and do not necessarily reflect those of the European Union or European Research Executive Agency (REA). Neither the European Union nor the granting authority can be held responsible for them."
• FCT / MCTES through national funds (PIDDAC) under the R&D Unit Institute for Sustainability and Innovation in Structural Engineering (ISISE), under reference UIDB / 04029/2020 (https://doi.org/10.54499/UIDB/04029/2020), and the Associate Laboratory Advanced Production and Intelligent Systems (ARISE) under reference LA/P/0112/2020.
• Universidad Politécnica de Madrid through grant 'Programa Propio', reference EST-PDI-25-0J77JO-37-NNVVUO, attributed to Jorge Conde.

References

[1] 'Global Status Report 2018: towards a zero-emission, efficient and resilient buildings and construction sector', International Energy Agency and the United Nations Environment Programme, 2018.
[2] Kanyilmaz, A., Birhane, M., and Fishwick, R., (2023). Reuse of Steel in the Construction Industry: Challenges and Opportunities. Int J Steel Struct, 23, 1399–1416.
[3] Ljubinković, F., Conde J., Janković. N., Simões da Silva L., (2024). 'Demountable reusable and adjustable moment-resisting joints for circular construction', 13th International Conference on Advances in Steel-Concrete Composite Structures (ASCCS 2024) Hong Kong, China.
[4] Simões, L., Ljubinković, F., Conde, J., Alves, T., J. F. Demonceau., J. F., Neutelers, A., Odenbreit, C., Bogdan, T., Mela, K., Bernabeu, A., González, G. (2023). CONNECT4C: High-strength steel connections for circular construction (RFCS-02-2022-RPJ, Deliverable D1.1 – Comprehensive overview of the project).
[5] Odenbreit, C., Yang, J., Romero, A., and Kozma, A. (2022). A reusable structural system fit for geometrical standardization and serial production. Ce/papers 5, 2.
[6] Silva, L.C., Tankova, T., Craveiro, H., Simões, R., Costa, R., and Simões, L. (2022). Behaviour of plug-and-play joints between RHS columns and CFS trusses. Structures, 41, 1719-1745.
[7] European Committee for Standardization, (2015). EN 14399-4:2015: High-strength structural bolting assemblies for preloading – Part 4: System HV – Hexagon bolt and nut assemblies. Brussels, Belgium.
[8] Jankovic, N., Ljubinković, F., Conde, J., Costa, J., & Simões, L. (2025). Behaviour and design resistance of long bolts in tension. J Constr Steel Res, 229, 109492.
[9] European Committee for Standardization (2005). EN 1993-1-8:2005: Eurocode 3: Design of steel structures - Part 1-8: Design of joints. Brussels, Belgium.